THE JOURNAL OF BIOLOGICAL CHEMISTRY VOL. 285, NO. 1, pp. 104–114, January 1, 2010

Proteomic Analysis of GLUT4 Storage Vesicles Reveals LRP1 to Be an Important Vesicle Component and Target of Insulin Signaling*[S]

Received for publication, July 2, 2009, and in revised form, October 23, 2009 Published, JBC Papers in Press, October 28, 2009, DOI 10.1074/jbc.M109.040428

Mark P. Jedrychowski[‡1], Carlos A. Gartner[§], Steven P. Gygi[§], Li Zhou[¶], Joachim Herz[¶], Konstantin V. Kandror[‡], and Paul F. Pilch[‡2]

From the [‡]Department of Biochemistry, Boston University Medical School, Boston, Massachusetts 02118, the [§]Department of Cell Biology, Harvard Medical School, Boston, Massachusetts 02115, and the [¶]Department of Molecular Genetics, University of Texas Southwestern Medical Center, Dallas, Texas 75390

Insulin stimulates the translocation of intracellular GLUT4 to the plasma membrane where it functions in adipose and muscle tissue to clear glucose from circulation. The pathway and regulation of GLUT4 trafficking are complicated and incompletely understood and are likely to be contingent upon the various proteins other than GLUT4 that comprise and interact with GLUT4-containing vesicles. Moreover, not all GLUT4 intracellular pools are insulin-responsive as some represent precursor compartments, thus posing a biochemical challenge to the purification and characterization of their content. To address these issues, we immunodepleted precursor GLUT4-rich vesicles and then immunopurified GLUT4 storage vesicle (GSVs) from primary rat adipocytes and subjected them to semi-quantitative and quantitative proteomic analysis. The purified vesicles translocate to the cell surface almost completely in response to insulin, the expected behavior for *bona fide* GSVs. In total, over 100 proteins were identified, about 50 of which are novel in this experimental context. LRP1 (low density lipoprotein receptor-related protein 1) was identified as a major constituent of GSVs, and we show it interacts with the lumenal domains of GLUT4 and other GSV constituents. Its cytoplasmic tail interacts with the insulin-signaling pathway target, AS160 (Akt substrate of 160 kDa). Depletion of LRP1 from 3T3-L1 adipocytes reduces GLUT4 expression and correspondingly results in decreased insulin-stimulated 2-[^{3}H]deoxyglucose uptake. Furthermore, adipose-specific LRP1 knock-out mice also exhibit decreased GLUT4 expression. These findings suggest LRP1 is an important component of GSVs, and its expression is needed for the formation of fully functional GSVs.

The insulin-dependent translocation of GLUT4 from intracellular membranes to the cell surface is a well studied paradigm for the effects of signal transduction on membrane trafficking, and this process is of considerable physiological relevance for the regulation of glucose homeostasis, as dysregulation of this process plays a role in insulin resistance and type 2 diabetes mellitus (1). Only about half of the intracellular GLUT4 translocates to the plasma membrane in response to insulin (2–5) suggesting that more than one GLUT4-containing compartment exists. In addition, kinetic analyses of GLUT4 trafficking are consistent with the interpretation that GLUT4 traffics through multiple intracellular compartments (6–8). These and other data have led to the concept that an ultimate target of insulin signaling is a subpopulation of translocating GLUT4-containing membranes that are commonly referred to as GLUT4 storage vesicles (GSVs)[3] (9, 10). The focus of many groups over the years has been on how these GSVs form, what their protein composition is, and how insulin communicates with them and stimulates their translocation to the cell surface.

GLUT4-containing vesicles have been purified and their protein composition analyzed by a number of investigators, first by conventional protein sequencing (11, 12) and more recently by mass spectrometry-based proteomic studies (13, 14). The initial studies identified the insulin-responsive aminopeptidase (IRAP) (11, 12) and the sorting receptor, sortilin (15, 16), as major proteins components of GLUT4 vesicles that translocate to the cell surface in response to insulin. With the advent of mass spectrometry, numerous additional proteins were identified as constituents of GLUT4-rich vesicles, notably components of the vesicular trafficking machinery (17) such as Vamp2 (13) and motor proteins that might mediate vesicle movement (18) as well as additional cargo proteins such as the receptors for transferrin (TfR) (13) and cation-independent mannose 6-phosphate (CIM6PR) (13, 18). Vamp2 had been shown previously to be a component of GLUT4 vesicles by immunological means (19). The receptors for TfR and CIM6PR were shown to be insulin-responsive by ligand binding studies (20, 21), but it was not clear if they were components of GLUT4-containing vesicles at that time. The limitation of the previous studies of GLUT4-enriched vesicles is that they analyzed the entire population of GLUT4-containing intracellular membranes and not

* This work was supported, in whole or in part, by National Institutes of Health Grant DK30435. This work was also supported by a grant from the American Diabetes Foundation (to P. F. P.).

[S] The on-line version of this article (available at http://www.jbc.org) contains supplemental Tables S1 and S2 and Figs. S1 and S2.

[1] Supported by National Institutes of Health Training Grant AG000115.

[2] To whom correspondence should be addressed. E-mail: ppilch@.edu.

[3] The abbreviations used are: GSV, GLUT4 storages vesicle; AS160, Akt substrate 160 kDa; CIM6PR, cation-independent mannose 6-phosphate; IRAP, insulin-responsive aminopeptidase; ICAT, isotope-coded affinity tag; LM, light microsomal; TfR, transferrin receptor; PBS, phosphate-buffered saline; MS, mass spectrometry; LC, liquid chromatography; MS/MS, tandem MS; shRNA, small hairpin RNA; PM, plasma membrane; PAI, protein abundance index; GST, glutathione *S*-transferase; PBS, phosphate-buffered saline; eGFP, enhanced green fluorescent protein.

just GSVs, the presumed end point target of insulin signaling. To purify GSVs, an immunological reagent that marks only GSV precursors is required, and such a reagent is a monoclonal antibody to cellugyrin (22).

Cellugyrin (23) is a member of the tetraspan family of vesicle membrane proteins that are ubiquitous components of membrane vesicles of as yet unknown function (24). Cellugyrin was identified as a component of GLUT4 vesicles by immunological means (22) and was shown to be present only in the ~50% of GLUT4-containing membranes that do not translocate to the cell surface (25). Here, we use an anti-cellugyrin monoclonal antibody to immunodeplete GSV precursor vesicles and then an anti-GLUT4 antibody to immunoisolate GSVs. Both populations were subjected to proteomic analysis, and over 100 proteins were identified. One of the most abundant proteins found in the proteomic analysis of GSVs was LRP1 (low density lipoprotein receptor-related protein 1), the largest member of the low density lipoprotein receptor gene family. LRP1 is involved in many physiological functions, including lipid and glucose metabolism, cellular entry of viruses and toxins, activation of lysosomal enzymes, cellular signal transduction, and neurotransmission (26). In this study, we analyze the distribution and trafficking of LRP1 in adipocytes and its interactions with GLUT4. We show that LRP1 is an important component of GSVs whose depletion in 3T3-L1 adipocytes has significant effects on GLUT4 expression and insulin-dependent glucose uptake and whose absence in mouse adipocytes also leads to GLUT4 deficiency.

EXPERIMENTAL PROCEDURES

Reagents—The following items were purchased from Sigma: dexamethasone, 3-isobutyl-1-methylxanthine, insulin, benzamidine, phosphatase inhibitor I and II, puromycin, ampicillin, 2-deoxyglucose, cytochalasin B, and fetal bovine serum (Australian origin). Aprotinin, leupeptin, and pepstatin A were obtained from American Bioanalytical (Natick, MA). Dulbecco's modified Eagle's medium was obtained from Mediatech, Inc. (Herndon, VA); 2-[^{3}H]deoxyglucose was purchased from PerkinElmer Life Sciences, and dimethyl pimelimidate·2HCl and disuccinimidyl suberate were purchased from Pierce. M-280 sheep anti-mouse, M-280 anti-rabbit Dynabeads, and calf serum were purchased from Invitrogen. Cleavable ICAT (isotope-coded affinity tags) reagent kit was purchased from Applied Biosystems (Foster City, CA). Sequencing grade modified trypsin was purchased from Promega (Madison, WI). Trans-IT 293 transfection reagent was obtained from Mirus (Madison, WI).

Antibodies to the following proteins were used: GLUT4 (3); IRAP (21st Century Biochemical, Hopkinton, MA); caveolin-1 (BD Transduction Laboratories, Lexington, KY); Vamp2 (Synaptic Systems, Germany); C/EBPα (Santa Cruz Biotechnology, Inc., Santa Cruz, CA); sortilin (Abcam, Cambridge, MA); transferrin receptor H68 (Zymed Laboratories Inc.); β-actin (Sigma), cellugyrin (Dr. Kostantin Kandror, Boston University School of Medicine, Boston); GLUT1 (Dr. C. Carter-Su, University of Michigan, Ann Arbor, MI); LRP1 (Dr. D. K. Strickland, University of Maryland School of Medicine, Baltimore); aP2 (Dr. D. Bernlohr, University of Minnesota); insulin-like growth factor receptor 2 (Dr. M. Czech, University of Massachusetts Medical School, Worchester); and Bap31 (Dr. G. Shore, McGill University, Montreal, Canada).

Cell Culture, shRNA Transfection, and Infection—Murine 3T3-L1 cells were cultured, differentiated, and maintained as described previously (27). Human embryonic kidney (HEK)-293T cells for lentivirus propagation were cultured in Dulbecco's modified Eagle's medium with 10% fetal bovine serum. LRP1 knockdown experiments were carried out using short hairpin RNA interference sequences. LRP1 mouse lentiviral (pLKO.1) vectors were purchased from Open Biosystems (Huntsville, AL) with the following sequences (Open Biosystems catalogue no. TRCN0000119622 to TRCN0000119625) (sense loop antisense): ccgggctgaacacattctttggtaa**ctcgag**ttaccaaagaatgtgttcagcttttg; ccgggcgaacaaatacactggctaa**ctcgag**ttagccagtgtatttgttcgcttttg; ccggcggagtcacttacatcaataa**ctcgag**ttattgatgtaagtgactccgttttg; and ccggcgcttgtgtattcccaagcat**ctcgag**atgcttgggaatacacaagcgttttg.

Forty percent confluent HEK293T cells (in a p150) were cotransfected with 24 μg of pLKO.1 LRP1 mouse lentiviral vector or pLKO.1 eGFP lentiviral vector containing 1.2 μg of TAT, 1.2 μg of REV, 1.2 μg of GAG/POL, 2.4 μg of VSV-G viral packaging plasmids using 90 μl of Trans-IT® 293 from Mirus (Madison, WI), and transfection conditions were followed as per the manufacturer's instructions. After 48 h, media were collected and filtered through a 45-μm pore size Whatman filter and was infected onto 3T3-L1 preadipocytes. After an additional 48 h post-infection, media were removed, and cells were selected with 1 μg/ml puromycin (Sigma) in 10% calf serum for an additional 48 h. LRP1 shRNA Target TRCN0000–119625 had the highest knockdown efficiency and was used for all subsequent studies, *i.e.* Western blotting, and 2-[^{3}H]deoxyglucose uptake assays were performed as described previously (27, 28).

Isolation and Fractionation of Rat Adipocytes—Primary rat adipocytes were isolated by collagenase digestion. Fractionation into cell surface and internal membranes was achieved by differential centrifugation as described previously (29, 30). The light microsomal fraction (1 mg of protein) was subjected to centrifugation in a 4.6-ml 10–30% (w/w) continuous sucrose gradient and spun at 250,000 × *g* in a Beckman Instruments (Palo Alto, CA) SW 55.1 rotor for 50 min at 4 °C. Fractions from the gradients were collected and analyzed for GLUT4 by gel electrophoresis and Western blot analysis prior to pooling of fractions for immunoadsorption.

Immunoadsorption of Cellugyrin and GLUT4-containing Vesicles—Protein A-purified monoclonal 1F8 (GLUT4) antibody, affinity-purified polyclonal cellugyrin (BIOSOURCE), as well as nonspecific mouse immunoglobulin G (50 μg each) were coupled to 500-μl Dynabeads M-280 sheep anti-mouse or anti-rabbit (Invitrogen) according to the manufacturer's instruction. Prior to use, the antibody-coupled beads were cross-linked with 1 ml of 20 mM dimethyl pimelimidate dihydrochloride (Pierce) in 0.2 M triethanolamine, pH 8.2, for 30 min at 20 °C. The reactions were quenched with 1 ml of 50 mM Tris, pH 7.5, for 15 min at 20 °C and washed three times with PBS. All subsequent steps were carried as described previously (25).

Cross-linking and Immunoprecipitation—Cross-linking of membrane proteins was performed as described (31). The isolated light microsomal (LM) (30) fraction (100 μg of protein) from rat epididymal fat was resuspended in 500 μl of PBS containing both protease and phosphatase inhibitors, and dithiobis(succinimidyl propionate) in DMSO was added to a final concentration of 2 mM for 30 min at 20 °C. The reaction was quenched with 50 mM Tris, pH 7.5, for 15 min at 20 °C, and solubilized with Triton X-100 to a final concentration of 1% for 30 min at 4 °C. Protein A/G (Santa Cruz Biotechnology) (50 μl) was coupled to either 5 μg of nonspecific mouse immunoglobulin G or 5 μg of protein A-purified monoclonal 1F8 GLUT4 antibody for 2 h at 4 °C in 1% Triton X-100 in PBS. The antibodies were coupled to protein A/G with dimethyl pimelimidate as described above for the immunoadsorption experiments. Cross-linked LM was then rotated with IgG beads for 2 h at 4 °C, and the supernatant was removed and further incubated with 1F8 GLUT4 beads for 2 h at 4 °C. Supernatants were removed, and beads were washed three times with 1% Triton X-100. Beads were eluted with 100 μl of Laemmli sample buffer for 30 min at 37 °C. Eluates were removed from the beads, and dithiothreitol was added to a final concentration of 50 mM and incubated for another 30 min at 37 °C. Equal proportions of eluate and supernatant were resolved by gel electrophoresis and analyzed by Western blotting.

Preparation of Whole Cell Extracts, Gel Electrophoresis, and Immunoblotting—Cultured cells were disrupted by ice-cold lysis buffer containing 50 mM Tris, pH 7.4, 100 mM NaCl, 1% sodium deoxycholate, 4% Nonidet P-40, 0.4% SDS, 1 mM pepstatin, 1 mM aprotinin, and 10 mM leupeptin; and phosphatase inhibitors I and II were added (Sigma). Lysates were vortexed and spun for 30 min at 16,000 $\times$ *g* in a microcentrifuge at 4 °C; supernatants were collected, and the protein concentrations were determined using the BCA kit (Pierce). Adipose tissue lysates from 8-week-old male LRP1 lox/lox mice and age-matched aP2Cre^{+}, LRP1 lox/lox mice (32) were prepared by grinding frozen tissue with a mortar and pestle in the above lysis buffer. Proteins were resolved by SDS-PAGE as described by Laemmli (33). Gels were transferred to polyvinylidene difluoride membranes pretreated with methanol (Bio-Rad) in 25 mM Tris, 192 mM glycine. Membranes were blocked with 10% nonfat dry milk in PBS containing 0.1% Tween 20 for 1 h at room temperature. Membranes were then probed with the primary antibodies for either overnight at 4 °C or 2 h at room temperature and incubated with horseradish peroxidase-conjugated secondary antibodies (Sigma). Signals were enhanced with chemiluminescent reagents (PerkinElmer Life Sciences) for detection of Western signals.

Plasmids—To generate the GST-fused C-terminal cytosolic tails for LRP1 and sortilin and N-terminal IRAP, the coding regions of each cytosolic domain were cloned from cDNA derived from epididymal fat pads of male Harlan Sprague-Dawley rats into a pGEX-5X-1 vector (GE Healthcare). The PCR cloning oligonucleotides (Invitrogen) are as follows: sense LRP1 cytosolic domain primer with an EcoRI restriction site, 5′-gatcgaattctgatcctctgctgc-3′, and an antisense primer with an XhoI restriction site, 5′-gatcctcgagctatgctaagggatcccc-3′; sense sortilin cytosolic domain primer with an EcoRI restriction site, 5′-gatcgaattcgtgaagaagtatgtctgt, and an antisense primer with an XhoI restriction site, 5′-gatcctcgagctattccaggaggtcctc-3′. All PCR products were digested with their corresponding restriction enzymes (New England Biolabs, Ipswich, MA) and ligated into their correspondingly digested pGEX-5X-1 vector.

LC-MS/MS Analysis—Samples were prepared for mass spectrometry by disulfide bond reduction and alkylation prior to separation by SDS-PAGE on precast 4–15% acrylamide gradient gels (Bio-Rad) and in-gel trypsin digestion as described (34). LC-MS/MS data were obtained using a LTQ Orbitrap (Thermo Fisher, San Jose, CA) mass spectrometer. Dried peptides were suspended in 10 μl of 5% acetonitrile, 3% acetic acid, and 4 μl were loaded onto a pulled fused silica microcapillary column (100 μm inner diameter, 12-cm bed) packed with C_{18} reverse phase resin (Magic C18AQ, 5-μm particles; 200 Å pore size; Michrom Bioresources, Auburn, CA). Peptides were resolved using an Agilent 1100 series binary pump across a 30-min linear gradient of 8–25% acetonitrile in 0.2% formic acid at a 250 nl/min flow rate. In each data collection cycle, one full MS scan (375–1600 *m/z*) was acquired in the Orbitrap (6×10^4 resolution setting; automatic gain control target of 10^6) followed by 10 data-dependent MS/MS scans in the LTQ (AGC target 5000; threshold 3000) using the 10 most abundant ions for collision-induced dissociation for fragmentation. The method dynamically excluded previously selected ions for 30 s, singly charged ions, and unassigned charged states.

Data Base Searching—Raw files obtained from the MS and MS/MS data collection were converted into mzXML format using the ReAdW program. Monoisotopic precursor ion and charge state information for each acquired MS/MS spectra were extracted by in-house software. The SEQUEST search algorithm was used to search the MS/MS spectra against the Mouse or Rat NCBI. The search parameters for post-translational modifications included a static modification of 57.02146 Da on cysteine (carboxyamidomethylation) and dynamic modification of 15.99491 Da for methionine (oxidation) residues. All peptides were based on the following filtering criteria: charge +1, Xcorr $\geq$2.0 $\Delta Cn \geq$0.01; charge +2, Xcorr $\geq$1.5 $\Delta Cn \geq$0.01; charge +3, Xcorr $\geq$2.0 $\Delta Cn \geq$ 0.03 with a mass accuracy $\pm$50 ppm. A given protein was considered correct (35) when >2 tryptic peptides were identified meeting or exceeding the aforementioned criteria.

For the c-ICAT labeling experiments (below), a static modification of 227.12699 Da cysteine (light) and dynamic modifications of 9.03019 Da (heavy) cysteine with the aforementioned Xcorr, ΔCn, and ppm parameters was used. Peptides pairs were submitted to quantitative analysis by an in-house software, VISTA, which has been described previously (36).

Cleavable ICAT (c-ICAT) Labeling and Purification—ICAT labeling of vesicle proteins was achieved as described previously (37). Heavy and light labeled immunoadsorptions were combined for IgG control and GLUT4 samples and loaded onto a 4–15% SDS-PAGE pre-cast gel (Bio-Rad) and stained with Coomassie Blue. Gels were subjected to in-gel trypsin digestion as described above. Peptides labeled with c-ICAT were purified with the avidin column supplied in the c-ICAT kit. Dried peptides were cleaved from their acid-labile moiety as recom-

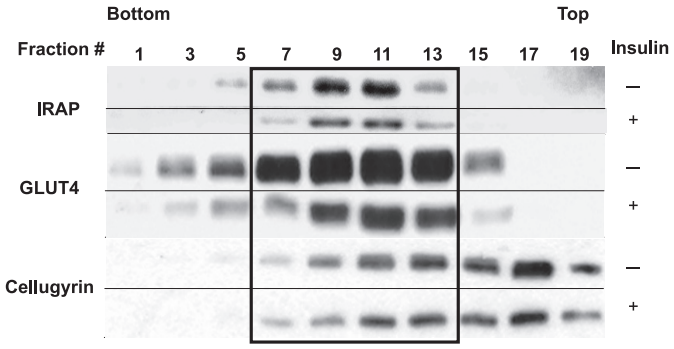

FIGURE 1. **IRAP, GLUT4, and cellugyrin have distinct distributions and insulin responsiveness.** Isolated rat adipocytes were treated with insulin or not and fractionated as described under "Experimental Procedures." The isolated light microsomal fraction (*LM*) (1 mg of protein) was separated into fractions by sucrose gradient centrifugation as described under "Experimental Procedures." *Odd-numbered* gradient fractions were immunoblotted for the proteins indicated, and detection was by enhanced chemiluminescence (*ECL*). The GLUT4/cellugyrin-enriched fractions were pooled (*outlined* in the *box*) and subjected to immunoadsorption as in Fig. 2. These data are representative of five separate experiments.

mended by the manufacturer and dried before nano-LC-MS/MS. IgG and GLUT4 samples were run in triplicate.

RESULTS

Purification of GSVs—In principle, vesicles can be immunoadsorbed directly from the light microsomal (LM) fraction of rat adipocytes, but mass spectral analysis following such a protocol revealed excessive cytoskeletal and ribosomal contaminants that complicated identification of vesicle proteins (data not shown). Accordingly, a sucrose gradient step was used first as shown in Fig. 1 where the *boxed part* of the gradient was concentrated and immunoadsorbed as shown in Fig. 2*A*. Both Figs. 1 and 2 reveal that cellugyrin does not significantly redistribute upon insulin stimulation, whereas GLUT4 and IRAP are markedly depleted from the LM fraction after insulin treatment. Quantitative analysis of the sequential immunoadsorption shows that 90% or greater of the GLUT4 and IRAP translocate from the cellugyrin-negative vesicles, and they translocate not at all or to a much lesser extent from the cellugyrin-positive vesicular pool (Fig. 2*B*). This nearly complete insulin-dependent redistribution of IRAP and GLUT4 is the expected behavior for *bona fide* GSVs. Thus, mass spectrometric analysis of the two immunoadsorbed fractions, before and after cellular insulin treatment, was used to identify their protein composition and determine the extent of protein translocation.

Semi-quantitative Proteomic Analysis Identifies >100 Proteins in GSVs and Precursor Vesicles—We classify the proteins we identified by mass spectrometry of immunoadsorbed vesicles (Fig. 3 and supplemental Table 1) into seven groups as shown in the *pie chart* of Fig. 3, and these proteins were all found in three or more individual mass spectrometry runs from independent experiments. We do not include ribosomal protein components in our data set, and we list in supplemental Table 2 as likely contaminants, proteins highly abundant in adipocytes such as caveolin-1 and several enzymes of lipid metabolism (fatty-acid synthase and acetyl-CoA carboxylase), as these bind to control IgG in significant amounts. We also exclude from Fig. 3 the nonabundant Rab GTPase proteins (38) because these bound equally or nearly so to the IgG-coupled beads as they did to the specific antibody-coupled beads (supplemental Table 2), although Rabs are *bona fide* components of GLUT4-containing vesicles (39). Many of the proteins we identified are novel in the context of prior studies of GLUT4 trafficking, and these are indicated as such in Fig. 3 and supplemental Table 1 by an *asterisk*. Fig. 3 features the presumed vesicular cargo proteins noting that the protein abundance index (PAI) value is the semi-quantitative index of relative abundance. The absolute PAI value gives an approximation of the comparative amounts, one protein to the next, and a decrease in value from basal to the insulin-stimulated GLUT4 immunoadsorption is indicative of hormone-dependent movement. Those labeled with # indicates translocation to the cell surface as verified by other means such as Western blotting. Note that the major GSV cargo proteins, IRAP, sortilin, and GLUT4, as well as other proteins, previously described as translocating in response to insulin treatment of adipocytes, namely the CIM6PR, TfR, and LRP1, were all detected and shown to translocate as determined by this protocol.

ICAT Labeling of GSVs Reveals the Translocation Behavior of 20 Proteins—In addition to the semi-quantitative analysis of Fig. 3 and the supplemental tables, we labeled GSVs with stable ICAT (40) to further monitor how insulin affects the protein composition of GSVs. The ICAT method is based on the post-isolation labeling of cysteine residues of proteins with chemically identical but differentially isotopically labeled reagents, isolation of tagged peptides after proteolysis, and their mass spectrometric quantification and sequence analysis (see supplemental Fig. 1 for a schematic). ICAT labeling gave us quantitative translocation values resembling what we would see if we performed Western blots for each of those proteins individually, although unlike the analysis of Fig. 3, it does not give any indication of protein-to-protein abundance. We found a much smaller number of ICAT-labeled proteins than proteins identified in the semi-quantitative experiments due to the fact that many proteins contain few (GLUT4) or no (many Snares) cysteine residues, and on average, only 1 in 10 tryptic peptides contains a cysteine. Nevertheless, as shown in Table 1, quantitative analysis of highly purified GSVs from primary rat adipose tissue reveals abundant proteins known to be GSV constituents, namely IRAP and sortilin, and they show translocation values comparable with those found in Fig. 2*B*. Strikingly, LRP1 had the most cysteine pairs identified with an average insulin translocation value of 80%, consistent with the results of Descamps *et al.* (41), and it was also identified as a highly abundant translocating protein in the semi-quantitative analysis (Fig. 3). LRP1 is a very large protein (~500 kDa) that would likely have eluded previous proteomic studies of GLUT4-containing vesicles (13, 14), because the SDS-PAGE analysis in these was performed with higher acrylamide concentrations and LRP1 would not have entered the gel under these circumstances. Note that several proteins that showed translocation as assessed by ICAT labeling, for example the adaptor proteins, are most likely showing insulin-dependent behavior unrelated to cell surface movement. In fact, they do not show this change in abundance as assayed by PAI (supplemental Table 1), and

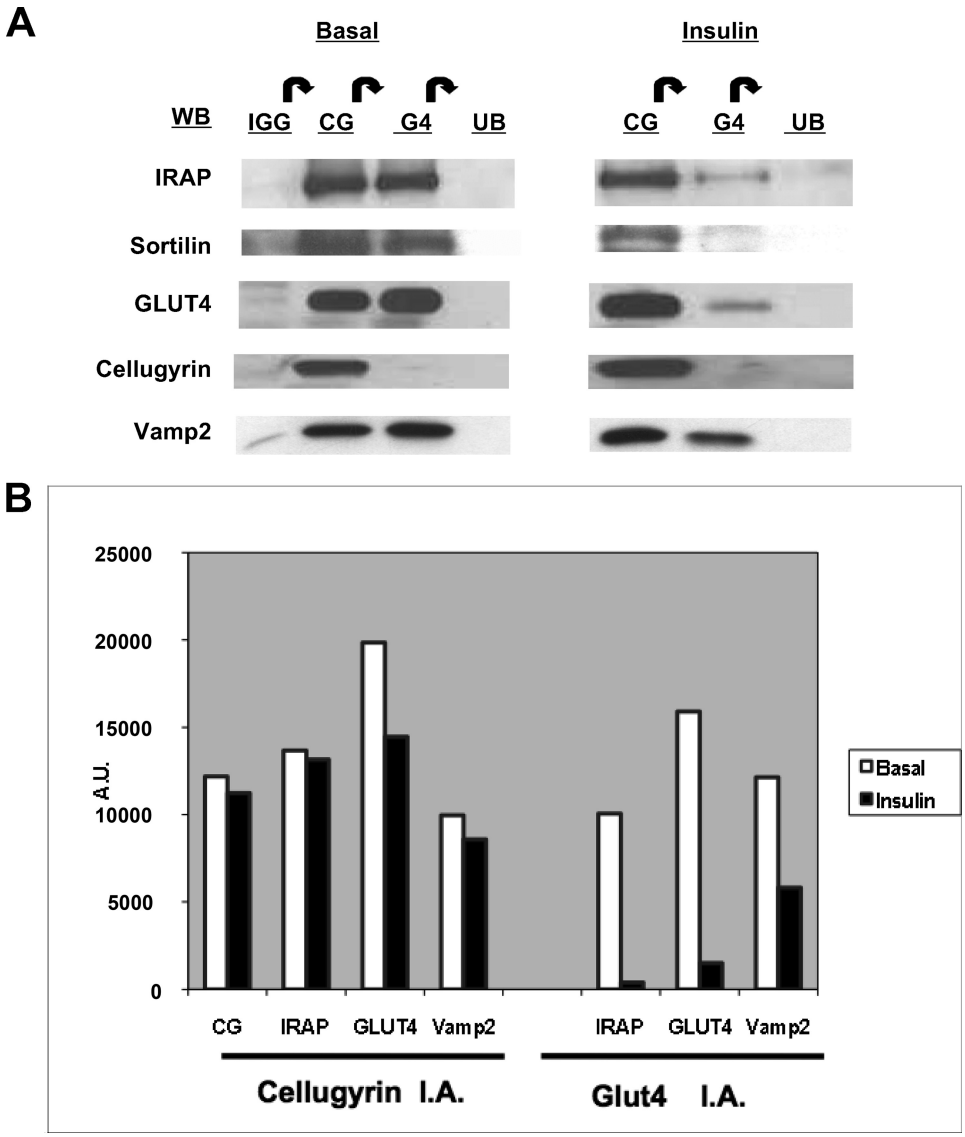

FIGURE 2. *A,* immunoadsorption of GLUT4-enriched sucrose gradient fractions show two distinction populations of GLUT4 vesicles. Separately pooled (as in Fig. 1) fractions for basal and insulin-treated rat adipocytes were precleared with anti-mouse IgG beads for 2 h, and the supernatants were immunoadsorbed with anti-cellugyrin (*CG*) beads for 2 h. Supernatants were collected and subjected to a subsequent GLUT4 (*G4*) immunoadsorption. All beads were washed three times with PBS, pH 7.4, and eluted with 100 μl of electrophoresis buffer. Equal proportions of IgG, cellugyrin, GLUT4, and supernatant were loaded on an SDS-polyacrylamide gel and analyzed by Western blot (*WB*) with proteins indicated as described under "Experimental Procedures." *B,* quantification of Western blots reveals GLUT4 vesicles depleted of cellugyrin translocate upon insulin stimulation. Relative amounts of cellugyrin (*CG*), IRAP, GLUT4, and Vamp2 were determined by scanning and analysis with NIH image software, and the results are represented graphically. These results are representative of experiments done five times. *A.U.*, arbitrary units; *I.A.*, immunoadsorption.

thus the changes we see in Table 1 are likely due to undetermined biochemical changes.

Fractionation of Primary Rat Adipocyte and Sucrose Velocity Gradient Fractionation Confirms LRP1 Translocates to the PM upon Insulin Stimulation—Because LRP1 was one of the most abundant proteins identified by proteomic analysis, Western blotting for LRP1 was performed to further validate its translocation and to assess its distribution upon insulin stimulation. Fig. 4, *A* and *B,* shows that LRP1 does indeed translocate to the PM upon insulin stimulation, and it is depleted from intracellular membranes. In addition, LRP1 was found to have the same sedimentation profile in a sucrose gradient as GLUT4 and IRAP (see Fig. 1), which could suggest that all three reside in the same or similar vesicles consistent with the immunoadsorption and mass spectrometry data. We identified the endoplasmic reticulum chaperone, Bap31 (42), as a moderately abundant protein component of cellugyrin-containing vesicles and other membranes (supplemental Table 1), and we use it in Fig. 4 as a loading control.

Translocation of TfR, CIM6PR, and LRP1 in Precursor GSVs and GSVs—It has been appreciated for some that the TfR (21, 29), cation-independent mannose 6-phosphate receptor (29, 43), and LRP1 (44) can translocate to the PM upon insulin stimulation in primary and cultured adipocytes. However, it has never been clear if this is due to their presence in GSVs or in other insulin-sensitive membrane compartments (45). Fig. 5, *A* and *B,* shows that the CIM6PR and TfR are primarily present in precursor GSVs, and they translocate mainly from the GSV compartment and to a much lesser degree than GLUT4. Their extent of translocation is consistent with the early studies of these proteins cited above that also showed a much smaller insulin-dependent translocation than that seen for GLUT4. However, LRP1 translocates to a significant extent from both precursor compartments consistent with the semi-quantitative and quantitative proteomic results.

LRP1 Directly Interacts with Sortilin, IRAP, and GLUT4—The LM fraction isolated from rat epididymal adipocytes was treated with the cross-linking agent, dithiobis(succinimidyl propionate). Dithiobis(succinimidyl propionate) is a homobifunctional, thiol-cleavable, and membrane-permeable cross-linker, which covalently links proteins by reacting with their lysine and/or N-terminal residues from a distance up to 12 Å. Moreover, IRAP, sortilin, and LRP1 have large ectodomains expressed in the lumen of intracellular vesicles, and if the domains interact, they may be detected by cross-linking. Thus, after exposure to dithiobis(succinimidyl propionate), membranes were solubilized, immunoprecipitated with anti-GLUT4 antibody (1F8), and blotted with antibodies for LRP1, IRAP, GLUT4,

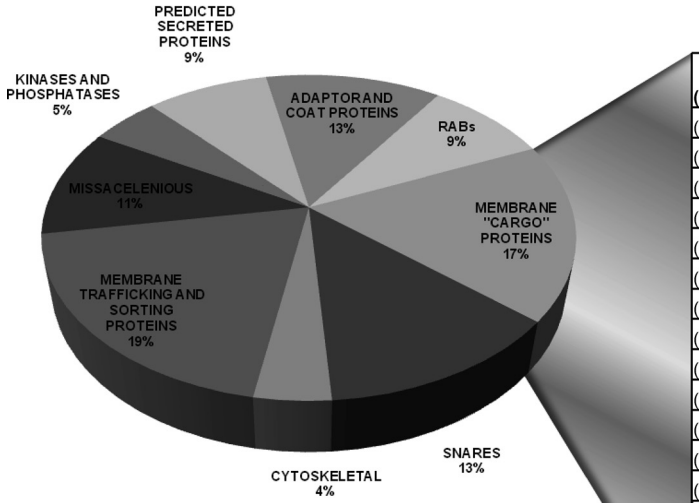

MEMBRANE "CARGO" PROTEINS

(GenBank Accession Number) Description	M.W.	Basal CG	Basal G4	Ins. CG	Ins. G4
(Q91ZX7) Lipoprotein Receptor Related Protein 1 # *	500 Kd	0.88	0.74	0.45	0.23
(Q63002)Mannose 6 Phosphate Recept./IGFII #	280 Kd	0.66	0.77	0.55	0.14
(O088307) Sortilin-Related LDLR Relative 11 *	247 Kd	0.22	0.44	0.23	0.18
(Q63632) ElectroNeutral K+/Cl- Cotransporter 1 *	120 Kd	0.16	0.24	0.14	0.12
(Q1Z1X1) vp115	120 Kd	0.18	0.22	0.18	0.44
(Q8C129) IRAP #	115 Kd	0.77	0.77	0.68	0.33
(P98156) VLDLR	96 Kd	0.18	0.33	0.15	0.22
(054861) Sortilin #	85 Kd	0.45	0.42	0.48	0.21
(P42893) Endothelin-Converting Enzyme *	86 Kd	0.05	0.29	0.07	0.18
(P07861) Neprilysin Neutral Endopeptidase *	79 Kd	0.04	0.14	0.05	0.22
(Q8CGU6) Nicastrin *	79 Kd	-	0.16	0.05	0.34
(Q9EPF2) Cell Surface Glycoprotein MUC18 *	71 Kd	0.05	0.52	0.04	0.14
(Q99376) Transferrin Receptor #	70 Kd	0.33	0.35	0.33	0.22
(P14142) GLUT4 #	55 Kd	0.48	0.48	0.48	0.23
(P26453) Basigin CD147 *	48 Kd	0.08	0.31	0.03	0.14
(Q6AY20) Cation-Dependent M6P Receptor #	40 Kd	0.33	0.33	0.33	0.14
(Q63691) Mono Differentiation Antigen CD14 *	39 Kd	0.09	0.21	0.08	0.15
(P27274) CD59 Glycoprotein *	13 Kd	0.06	0.06	0.08	0.07

FIGURE 3. **Classes of proteins identified in precursor GSV and GSV compartments.** Proteins found were categorized according to their presumed function as indicated in the *pie chart* (see supplemental Tables S1 and S2 for a complete list of all proteins identified). Details are given for presumptive cargo proteins in the *table* part of the figure as some of these are known GSV components (indicated by *). Relative protein abundance between the various immunoadsorption conditions were calculated by PAI as described (69). This index is based on the ratio of actual tryptic peptides identified by mass spectrometry divided by the theoretical tryptic peptides index within the mass range of 700–2600 Da, and the higher the number, the more abundant the protein. The *table* shows data from one of five similar experiments.

TABLE 1

Quantitation data of ICAT-labeled GSVs

Immunoadsorbed GSVs were isolated, ICAT-labeled, SDS-PAGE-resolved, digested with trypsin, analyzed by LC-MS/MS, identified with SEQUEST software, and quantified with VISTA software as described under "Experimental Procedures." Proteins were categorized according to the number of cysteine ICAT-labeled pairs identified. The percent translocation values for basal GSVs was calculated for each protein from the averages of cysteine-labeled peptide VISTA values in the three LC-MS/MS runs in addition to their corresponding standard deviation values. HDL, high density lipoprotein; TPPC, trafficking protein particle complex.

Name	Uniprot kb/ Swiss-Prot accession no.	Cysteine pairs	Translocation from basal GSVs	S.D.
			%	%
LRP1	Q91ZX7	11	80	4
Clathrin	Q68FD5	10	22.5	201
Sortilin	O54861	5	70	4.5
CIM6PR	Q07113	4	29	9.2
IQGAP1	Q9JFK1	4	34.2	23.7
VPS35	Q9EQH3	4	49	4.6
IRAP	Q64514	4	78	5.9
AP complex 2 a2	P18484	3	55	9.9
AP complex 2 a1	Q9DBG3	3	70	15
Cation-dependent Man-6-P receptor	Q6AY20	2	31	10
Lipin-1	Q14693	2	73	3
TPPC subunit 3	O55013	1	31	8.3
Electroneutral K^+/Cl^- co-transporter 1	Q63632	1	32.9	14.8
Myotonic dystrophy kinase	O54875	1	32.9	32.9
TMP21	Q8R1V4	1	39	11
Synaxin 12/13	O70319	1	44.1	10.1
Vigilin HDL-binding protein	Q9Z1A6	1	55	10.8
Cell surface glycoprotein MUC18	Q9EPF2	1	67	9.9

cellugyrin, and protein-disulfide isomerase followed by SDS-PAGE under reducing conditions. As shown in Fig. 6, LRP1, IRAP, sortilin, and GLUT4 co-immunoprecipitated, whereas cellugyrin and protein-disulfide isomerase, an abundant oxidoreductase enzyme found in the endoplasmic reticulum, did not. Cellugyrin contains a small lumenal domain (46), and we would not expect a direct interaction with GLUT4 under the aforementioned immunoprecipitation conditions.

Lentiviral shRNA Knockdown of LRP1 Results in a Decreased Expression of IRAP, Sortilin, and GLUT4 in 3T3-L1 Adipocytes—During 3T3-L1 adipocyte differentiation, LRP1 shows a slight increase in expression (data not shown) similar to that of IRAP but to a much lesser degree than GLUT4 and sortilin (47). To see how LRP1 expression affected GSV formation, we created three stable cell lines expressing LRP1-directed shRNA in a lentivirus vector. Expression of two target sequences resulted in a modest (40–60%, data not shown) decrease in LRP1 protein levels, although a third gives a significant (≥90%) ablation of the LRP1 signal as shown in Fig. 7. These cells were monitored for the expression of GLUT4, IRAP, and sortilin, all of which were significantly decreased by LRP1 knockdown (Fig. 7). On the other hand, an increase in GLUT1 expression was seen with abundant adipocyte proteins, caveolin-1 and aP2 being unchanged as were the levels of cellugyrin and β-actin. As a further control for any effect on adipocyte differentiation, peroxisome proliferator-activated receptor γ protein was also assessed and shown to be relatively unchanged (Fig. 7), and the adipocytes expressing the shRNA appeared identical to the controls in size, shape, and fat droplet content (data not shown). To determine whether LRP1 knockdown affected mRNAs for the vesicle proteins whose expression changed, we performed quantitative PCR (supplemental Fig. S2). This analysis shows a parallel change in protein and mRNA levels with GLUT4, IRAP, and sortilin being reduced and GLUT1 being increased at both levels. Given that LRP1 knockdown reduces the amount of the most abundant constituents of precursor

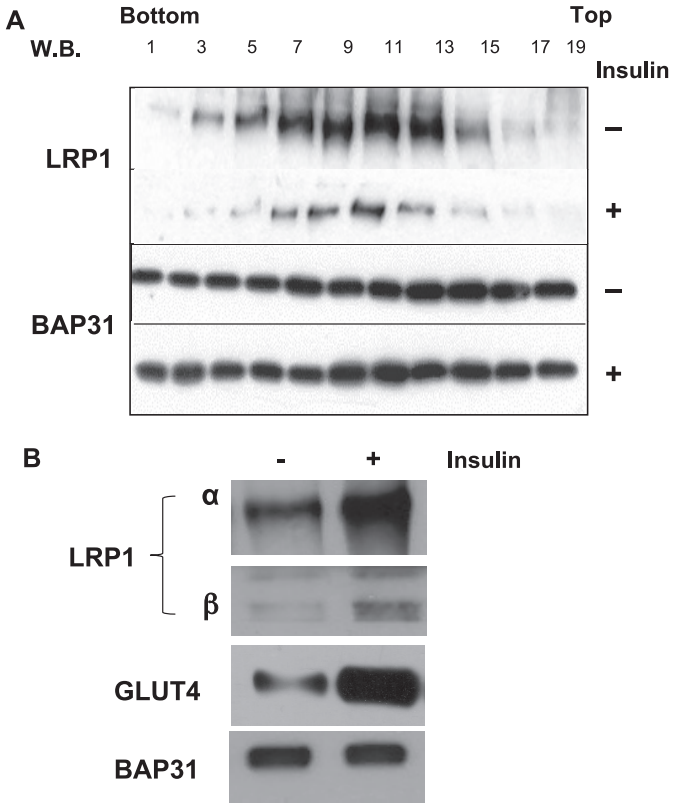

FIGURE 4. *A,* LM sucrose velocity gradient of LRP1 shows a similar sedimentation pattern to other GSV cargo. Sucrose sedimentation gradients were performed as described in Fig. 1 except for the Western blotting (*W.B.*) when a 4% SDS-PAGE was used to resolve the proteins prior to transfer. The chaperone protein BAP31 is shown as a loading control. *B,* insulin-stimulated translocation of LRP1 and GLUT4 to the PM. Fractionation of rat epididymal adipose tissue was performed as described under "Experimental Procedures." PM (10 μg) was used for Western blotting of the indicated proteins, which were detected as in previous figures.

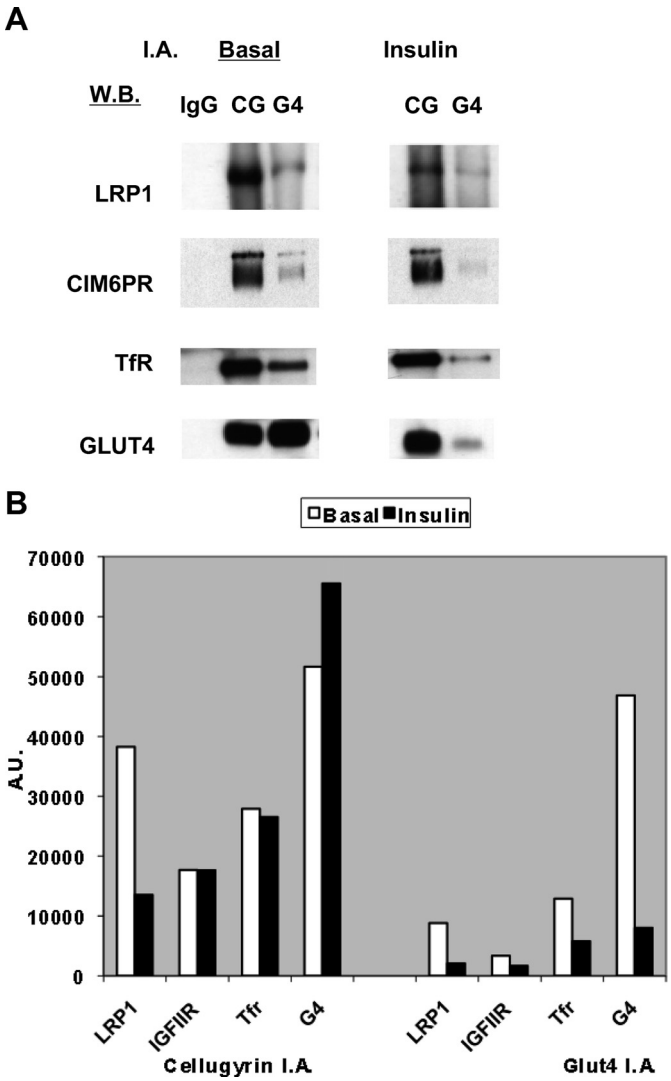

FIGURE 5. *A,* immunoadsorption of precursor GSVs and GSVs reveals CIM6PR, TfR, and LRP1 translocate upon insulin stimulation. Pooled sucrose gradient fractions were sequentially immunoadsorbed (*I.A.*) as described under "Experimental Procedures" and blotted for the proteins indicated as in previous figures. The results are representative of three independent experiments. *B,* Western blot (*W.B.*) quantitation of immunoadsorptions. The relative amounts of LRP1, IGFIIR, TfR, and GLUT4 (*G4*) were quantified by scanning and analysis with NIH image software and represented graphically. *CG*, cellugyrin; *A.U.*, arbitrary units.

GSVs and/or GSVs, we performed further analysis of basal and insulin-dependent 2-[^{3}H]deoxyglucose uptake.

Insulin-stimulated 2-[^{3}H]Deoxyglucose Uptake Is Decreased in LRP1-depleted 3T3-L1 Adipocytes—As shown in Fig. 8, eGFP-transfected control cells exhibit a 4-fold increase in insulin-stimulated glucose uptake, whereas the LRP1 knockdown cell line shows an increase of 1.8-fold. Because insulin-stimulated glucose transport correlates with GLUT4 expression in cultured adipocytes (48), this decreased transport is very likely to be a direct result of the decreased amount of GLUT4 present in these cells as shown in Fig. 7. In addition, although statistically insignificant, a slight increase in basal 2-[^{3}H]deoxyglucose is seen for the LRP1-deficient cell line compared with the control basal, which may be attributed to the increase in GLUT1 expression found in the LRP1 shRNA cells.

Epididymal Adipose Tissue from Lrp1 Adipose-specific Knock-out Mice Show Decreased Expression of GLUT4 and Sortilin—An *Lrp1* gene knock-out in mice is embryonically lethal, but an LRP1 adipose tissue-specific knock-out mouse has been created and characterized to be resistant to dietary fat-induced obesity and has improved glucose tolerance due to secondary muscle effects (32). This whole animal study did not, however, assess fat cell glucose transport *in vitro* nor did a more recent study of adipocyte differentiation from *Lrp1*$^{-/-}$ fibroblasts (49). Thus, to assess the direct effects of LRP1 deficiency in these mice on GSV components, we determined GLUT4 expression by Western blot as shown in Fig. 9. GLUT4 levels did indeed decrease in the epididymal fat tissues consistent with our LRP1 shRNA data, and in addition sortilin expression was also decreased.

LRP1 C Terminus Binds Akt Substrate of 160 kDa (AS160)—The Rab Gap, AS160, plays an important role in insulin-dependent GLUT4 trafficking (50), and it has been shown to bind to IRAP in pulldown (51) and vesicle adsorption experiments (52). The intracellular sequence of LRP1 has homologies to that of IRAP, and accordingly, we performed pulldown experiments with cytosolic sequences from IRAP, sortilin, and LRP1, and we blotted for AS160 as show in Fig. 10. Interestingly, IRAP and LRP1 constructs pulled down AS160 from insulin-stimulated cytosol, whereas sortilin did not, and the p115 pulldown is

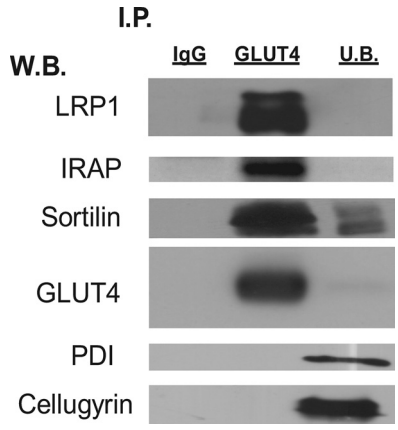

FIGURE 6. **Reversible cross-linking of LM and immunoprecipitation (*I.P.*) by GLUT4 reveals a direct interaction between GSV proteins LRP1, IRAP, sortilin, and GLUT4.** Primary rat adipocytes were fractionated as described under "Experimental Procedures." A modified version (70) of cross-linking was performed. The isolated LM fraction (100 μg of protein) from rat epididymal fat was resuspended in 500 μl of PBS containing both protease and phosphatase inhibitors, and dithiobis(succinimidyl propionate) was added to a final concentration of 2 mM for 30 min at 20 °C. The samples were processed as described under "Experimental Procedures" and resolved by SDS-PAGE, transferred, and blotted for the indicated proteins. Detection was by ECL. *PDI*, protein-disulfide isomerase; *W.B.,* Western blot; *U.B.,* unbound.

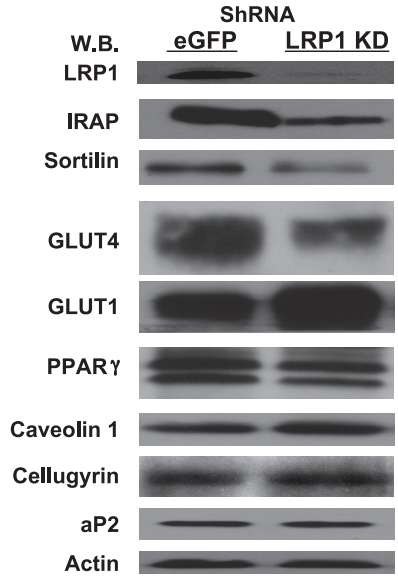

FIGURE 7. **LRP1 depletion in 3T3-L1 adipocytes show decreased expression of IRAP, sortilin, and GLUT4.** LRP1 and control eGFP stable knockdown 3T3-L1 fibroblasts were differentiated as described under "Experimental Procedures." Cells were harvested, and whole cell extracts were prepared as described under "Experimental Procedures." Protein (50 μg) was resolved by SDS-PAGE and Western blotted (*W.B.*) for the proteins shown. Detection was by enhanced chemiluminescence, and a representative blot is depicted. *PPAR,* peroxisome proliferator-activated receptor.

shown as a known partner of IRAP (53) that also binds to the other two proteins. That AS160 could be pulled down by the LRP1 intracellular domain was also confirmed by mass spectrometry (data not shown).

DISCUSSION

We report the following novel observations in this study. 1) We isolate vesicles with the properties of *bona fide* GSVs and describe their protein composition in terms of >100 constituent proteins, many of them not previously known in this context. 2) We determine that the insulin-dependent translocating proteins, including the CIM6P and transferrin receptors, translocate mainly from the GSV compartment. 3) Importantly, we find that LRP1 is a major GSV cargo protein whose expression *in vitro* and *in vivo* is necessary for fully functional GSVs and insulin-stimulated glucose uptake. 4) We show that LRP1 is a target of insulin signaling. Collectively, these data have important implications for the ontogeny of the GSV compartment and how it interacts with the insulin-signaling pathway. The conclusions we derive from our analyses may also have general utility in considering how another vesicle trafficking paradigm might arise, namely vasopressin-sensitive, aquaporin 2-rich vesicles of the kidney collecting duct.

LRP1 is an essential protein in mice as deletion of the *Lrp1* gene is embryonically lethal (54), a result consistent with its pleiotropic role in signaling and lipoprotein metabolism in many tissues (55). LRP1 is expressed in cultured adipocytes and has been shown to translocate from intracellular compartments to the cell surface upon insulin stimulation (44, 56). Indeed, LRP1 was also known to show insulin-sensitive trafficking in primary adipocytes as shown by ligand binding assays (41), but its location in GSVs was not investigated in these prior studies. Adipocyte-specific LRP1$^{-/-}$ mice display abnormalities of lipid clearance and energy balance *in vivo* (32, 49). Our data showing decreased GLUT4 expression in adipocytes from the tissue-specific knock-out (Fig. 9) offer a mechanistic explanation, at least in part, for this phenotype because lipid storage requires adequate glucose transport to form the triglyceride backbone upon glycolysis, and this process would be compromised in the knock-out adipocytes. Our *in vitro* data showing that LRP1 knockdown reduces GLUT4 levels and insulin-dependent glucose transport also support this hypothesis (Figs. 7 and 8). A second interesting aspect of the role of LRP1 in adipocytes is its ability to bind AS160 (57), a major target of insulin signaling (Fig. 10). A number of adaptor proteins have previously been shown to bind to the cytosolic sequence of LRP1 (58), including components of several other signaling pathways (55), and thus our results are consistent with these data and support a role for LRP1 in insulin signaling to GSV translocation.

The role of LRP1 in altering the expression of GLUT4 and other GSV constituents also gives further insight into the formation and trafficking of GSVs. Shi *et al.* (59) proposed a model for the formation of these vesicles based on the interactions of the lumenal domains of GLUT4, sortilin, and IRAP, the major GSV protein constituents known when their studies were completed. The mass spectrometry data of Fig. 3 and Table 1 show that LRP1 is also one of the more abundant proteins in GSVs, similar in amount to IRAP (25) by these criteria, and its very large size would easily lend itself to extensive interactions with the lumenal domains of the other GSV constituents. Indeed, the cross-linking data of Fig. 6 that show all four major GSV proteins can interact and the fact that diminishing the amounts of LRP1 *in vitro* and *in vivo* reduces the levels of GLUT4 together are consistent with the idea that a self-assembling mechanism applies to GSVs (59). However, the hierarchy of events in this process, *i.e.* who binds what and when during vesicle formation and trafficking, may need reexamination in the light of the

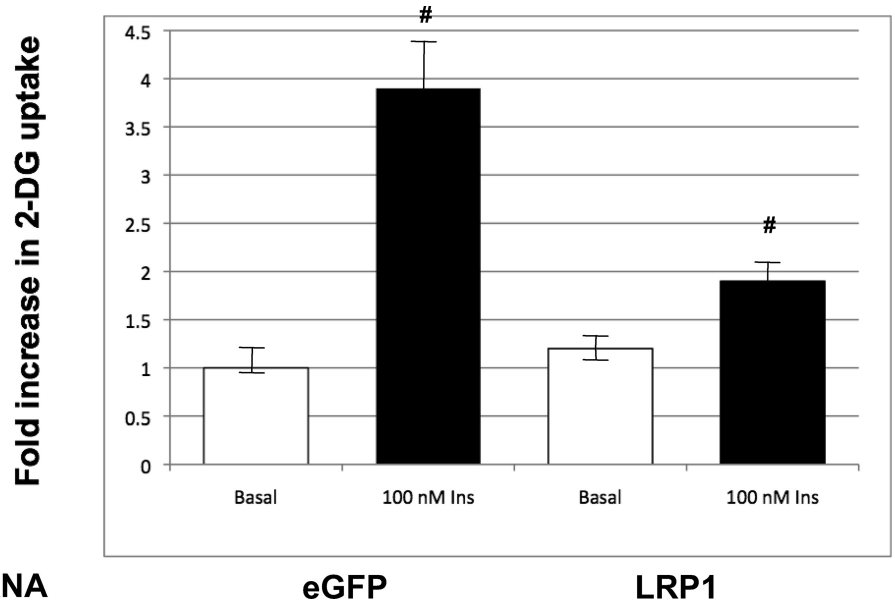

FIGURE 8. **LRP1-depleted 3T3-L1 adipocytes show a decrease in insulin-stimulated 2-[^{3}H]deoxyglucose uptake.** Assays were performed in 6-well plates as described under "Experimental Procedures." 2-[^{3}H]Deoxyglucose (*2-DG*) counts were normalized to basal eGFP-transfected cells, and fold insulin-stimulation was assessed for each cell line. The results are presented as the mean ± S.D. for averaged duplicates from three separate experiments (# denotes $p \leq 0.05$ and eGFP *versus* LRP1 shRNA).

FIGURE 9. **Epididymal adipose tissues from LRP1 adipose-specific knockout (*KO*) mice show decreased expression of GLUT4 and sortilin.** Epididymal adipose tissues were isolated from 8-week-old male LRP1 lox/lox mice and an 8-week-old male aP2Cre$^+$, LRP1 lox/lox mice. Cell lysates from the adipose tissues were prepared as described under "Experimental Procedures." Proteins (25 μg) were resolved by SDS-PAGE, followed by Western blotting for the indicated proteins. The GLUT4 data were confirmed in a second animal pair (data not shown). *WT*, wild type; *GAPDH*, glyceraldehyde-3-phosphate dehydrogenase.

LRP1 data. It is also worth noting that the cytosolic sequence of LRP1 has both dileucine- and tyrosine-based sorting motifs (60), the former in common with all other abundant GSV cargo components. Moreover, both LRP1 and IRAP bind AS160 (Fig. 10), although the residues on these proteins mediating this interaction have not been mapped.

The mechanism by which LRP1 knockdown reduces the amount of GLUT4 protein expression (Fig. 7) is not clear as the cognate mRNA is also correspondingly reduced as are those for IRAP and sortilin (supplemental Fig. S2). Aside from their co-localization in GSVs, these proteins have no obvious common feature that governs their expression as the latter two are expressed in many tissues where GLUT4 is not. This underscores the global regulatory role of LRP1 in many tissues (55), including adipocytes *in vivo* (32).

The fact that GSVs are insulin-sensitive, tissue-specific compartments, characteristic of fat and striated muscle tissue where postprandial glucose transport is tightly regulated, has fostered the idea that there likely exist proteins other than GLUT4 with a similar or identical tissue distribution that underlie the unique regulation and behavior of these vesicles. We now add over 50 proteins to the list of possible players in this regard (Fig. 3 and supplemental Table 1), but none of these has an obvious function or tissue distribution that could account for the observed vesicle properties, except for GLUT4. We cannot rule out, however, that we failed to detect a critical protein(s) of low abundance that functions in this regard. Nevertheless, our data raise the issue of how GSVs come to exist with the protein composition we find. Based on the fact that some constituent proteins of GSVs are present at the cell surface and cycle to and from the cell interior in a constitutive manner early in the process of differentiation, but then become sequestered intracellularly as GLUT4 and other vesicle proteins become highly expressed later in the process (28), it was postulated that vesicle formation was driven by mass action (10) in the following way. In fibroblasts, vesicular traffic is largely constitutive. The differentiation process results in the expression of protein(s) that block vesicle movement to the cell surface, and it is one or more of these proteins that is a target of insulin signaling that allows GSV exocytosis. This target or targets may have a tissue-specific expression pattern, but their identification remains to be made. Although AS160 is one such target, compromising its activity or expression only partially recapitulates the effects of insulin suggesting that there are other important Akt substrates (see below) (13, 50). Thus, proteins such as sortilin and GLUT4 that are expressed at high levels late in differentiation need to find a resident membrane, and they are targeted to existing vesicles and cause the formation of more and more such vesicles that accumulate IRAP, LRP1, and many other proteins (Fig. 3 and supplemental Table 1). Overexpression of GLUT4 has been shown to increase the number of GLUT4-containing vesicles

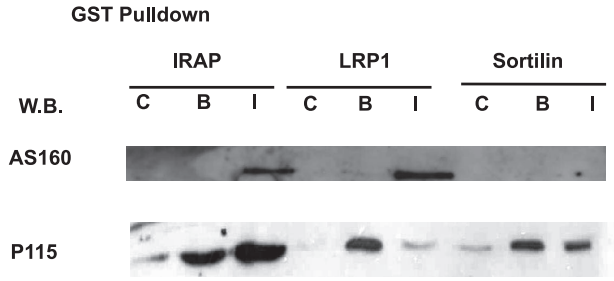

FIGURE 10. **GST pulldowns containing the cytosolic domains of IRAP, sortilin, and LRP1 reveal its interactions with P115, and AS160.** GST plasmids were constructed, induced, and purified as described under "Experimental Procedures." Rat adipocytes were treated with 100 nM insulin or not and fractionated as described under "Experimental Procedures." The cytosolic fraction (1 mg) from rat adipocytes stimulated (*I*) or not (*B*) with 100 nM insulin were precipitated with GST (*C*), GST-IRAP fusion protein (*IRAP*), GST-LRP1 fusion protein (*LRP*), and GST-sortilin fusion protein (sortilin) as described under "Experimental Procedures." Pulldowns were subjected to SDS-PAGE, transferred onto a polyvinylidene difluoride membrane, and Western blotted (*W.B.*) for the indicated proteins.

(61) consistent with the mass action hypothesis. Moreover, it is striking that vasopressin-sensitive aquaporin-2 containing vesicles that regulate water retention in the collecting duct of the kidney have many of the same protein constituents as GSVs, including IRAP, sortilin, and both mannose 6-phosphate receptors, as well as many or all of the same membrane trafficking machinery components that might be expected (62). Thus, the mass action and self-assembly model may be a common pathway for the formation of several types of tissue-specific, regulated vesicular traffic.

We can compare our results to those of Larance *et al.* (13) who employed vesicle isolation from cultured adipocytes followed by mass spectrometry and note that we identified almost every protein they did with the notable exception of AS160, which we identified only in pulldown assays (Fig. 10). This discrepancy may be due to technical details and/or the differences between primary and cultured adipocytes. Proteins identified in common include cargo proteins (Fig. 3 and Table 1), Snares and Rabs (supplemental Tables S1 and S2), and components of the retromer complex (supplemental Table S1) that mediates endosome to Golgi retrograde traffic (63). We also identified in reasonable abundance the tetraspan vesicle membrane proteins of the secretory component-associated membrane proteins, physin, and gyrin families (24), all of which had been previously identified as participating in GLUT4 trafficking by immunological means (22, 64, 65). These were also not seen by Larance *et al.* (13) possibly for the same reasons noted above.

The identity of the Rab involved in GSV exocytosis has remained controversial and ambiguous as many Rabs have been implicated at some stage of GLUT4 trafficking. In this study, we identified a number of Rab proteins, but they are not enriched in GSVs (supplemental Table 2) nor have any of them been definitively linked to GSV exocytosis (39). Another mystery is the identity of the target(s) for Akt, other than AS160, that is involved in GSV movement. In this regard, the data of others suggesting that one or more such targets may be at or near the plasma membrane (66, 67) are consistent with the lack of obvious candidates in our proteomic analysis of vesicle proteins. As for cargo protein, we identified by semi-quantitative mass spectrometry, the sortilin-related receptor, SORL1 (68), as a relatively abundant, apparently translocating, protein of GSVs (Fig. 3). An association of SORL1 with Alzheimer disease has been established (68), and this protein has not previously been described in adipocytes. Therefore, it is an attractive target for further study in the context of the physiology of these cells and GSV function.

REFERENCES

1. Huang, S., and Czech, M. P. (2007) *Cell Metab.* **5,** 237–252
2. Zorzano, A., Wilkinson, W., Kotliar, N., Thoidis, G., Wadzinkski, B. E., Ruoho, A. E., and Pilch, P. F. (1989) *J. Biol. Chem.* **264,** 12358–12363
3. James, D. E., Brown, R., Navarro, J., and Pilch, P. F. (1988) *Nature* **333,** 183–185
4. Cushman, S. W., and Wardzala, L. J. (1980) *J. Biol. Chem.* **255,** 4758–4762
5. Holman, G. D., Kozka, I. J., Clark, A. E., Flower, C. J., Saltis, J., Habberfield, A. D., Simpson, I. A., and Cushman, S. W. (1990) *J. Biol. Chem.* **265,** 18172–18179
6. Yang, J., and Holman, G. D. (1993) *J. Biol. Chem.* **268,** 4600–4603
7. Yeh, J. I., Verhey, K. J., and Birnbaum, M. J. (1995) *Biochemistry* **34,** 15523–15531
8. Lee, W., Ryu, J., Spangler, R. A., and Jung, C. Y. (2000) *Biochemistry* **39,** 9358–9366
9. Rea, S., and James, D. E. (1997) *Diabetes* **46,** 1667–1677
10. Pilch, P. F. (2008) *Acta Physiol.* **192,** 89–101
11. Kandror, K. V., and Pilch, P. F. (1994) *Proc. Natl. Acad. Sci. U.S.A.* **91,** 8017–8021
12. Keller, S. R., Scott, H. M., Mastick, C. C., Aebersold, R., and Lienhard, G. E. (1995) *J. Biol. Chem.* **270,** 23612–23618
13. Larance, M., Ramm, G., Stöckli, J., van Dam, E. M., Winata, S., Wasinger, V., Simpson, F., Graham, M., Junutula, J. R., Guilhaus, M., and James, D. E. (2005) *J. Biol. Chem.* **280,** 37803–37813
14. Guilherme, A., Emoto, M., Buxton, J. M., Bose, S., Sabini, R., Theurkauf, W. E., Leszyk, J., and Czech, M. P. (2000) *J. Biol. Chem.* **275,** 38151–38159
15. Lin, B. Z., Pilch, P. F., and Kandror, K. V. (1997) *J. Biol. Chem.* **272,** 24145–24147
16. Morris, N. J., Ross, S. A., Lane, W. S., Moestrup, S. K., Petersen, C. M., Keller, S. R., and Lienhard, G. E. (1998) *J. Biol. Chem.* **273,** 3582–3587
17. Thurmond, D. C., and Pessin, J. E. (2001) *Mol. Membr. Biol.* **18,** 237–245
18. Bose, A., Guilherme, A., Huang, S., Hubbard, A. C., Lane, C. R., Soriano, N. A., and Czech, M. P. (2005) *J. Biol. Chem.* **280,** 36946–36951
19. Mastick, C. C., and Falick, A. L. (1997) *Endocrinology* **138,** 2391–2397
20. Appell, K. C., Simpson, I. A., and Cushman, S. W. (1988) *J. Biol. Chem.* **263,** 10824–10829
21. Tanner, L. I., and Lienhard, G. E. (1987) *J. Biol. Chem.* **262,** 8975–8980
22. Kupriyanova, T. A., and Kandror, K. V. (2000) *J. Biol. Chem.* **275,** 36263–36268
23. Janz, R., and Südhof, T. C. (1998) *J. Biol. Chem.* **273,** 2851–2857
24. Hübner, K., Windoffer, R., Hutter, H., and Leube, R. E. (2002) *Int. Rev. Cytol.* **214,** 103–159
25. Kupriyanova, T. A., Kandror, V., and Kandror, K. V. (2002) *J. Biol. Chem.* **277,** 9133–9138
26. Herz, J., and Strickland, D. K. (2001) *J. Clin. Invest.* **108,** 779–784
27. Stephens, J. M., Lee, J., and Pilch, P. F. (1997) *J. Biol. Chem.* **272,** 971–976
28. El-Jack, A. K., Kandror, K. V., and Pilch, P. F. (1999) *Mol. Biol. Cell* **10,** 1581–1594
29. Kandror, K. V., and Pilch, P. F. (1998) *Biochem. J.* **331,** 829–835
30. Simpson, I. A., Yver, D. R., Hissin, P. J., Wardzala, L. J., Karnieli, E., Salans, L. B., and Cushman, S. W. (1983) *Biochim. Biophys. Acta* **763,** 393–407
31. Pilch, P. F., and Czech, M. P. (1979) *J. Biol. Chem.* **254,** 3375–3381
32. Hofmann, S. M., Zhou, L., Perez-Tilve, D., Greer, T., Grant, E., Wancata, L., Thomas, A., Pfluger, P. T., Basford, J. E., Gilham, D., Herz, J., Tschöp, M. H., and Hui, D. Y. (2007) *J. Clin. Invest.* **117,** 3271–3282
33. Laemmli, U. K. (1970) *Nature* **227,** 680–685
34. Li, X., Gerber, S. A., Rudner, A. D., Beausoleil, S. A., Haas, W., Villén, J., Elias, J. E., and Gygi, S. P. (2007) *J. Proteome Res.* **6,** 1190–1197
35. Elias, J. E., Haas, W., Faherty, B. K., and Gygi, S. P. (2005) *Nat. Methods* **2,** 667–675

36. Bakalarski, C. E., Elias, J. E., Villén, J., Haas, W., Gerber, S. A., Everley, P. A., and Gygi, S. P. (2008) *J. Proteome Res.* **7,** 4756–4765
37. Ramus, C., Gonzalez de Peredo, A., Dahout, C., Gallagher, M., and Garin, J. (2006) *Mol. Cell. Proteomics* **5,** 68–78
38. Jordens, I., Marsman, M., Kuijl, C., and Neefjes, J. (2005) *Traffic* **6,** 1070–1077
39. Watson, R. T., and Pessin, J. E. (2006) *Trends Biochem. Sci.* **31,** 215–222
40. Gygi, S. P., Rist, B., Gerber, S. A., Turecek, F., Gelb, M. H., and Aebersold, R. (1999) *Nat. Biotechnol.* **17,** 994–999
41. Descamps, O., Bilheimer, D., and Herz, J. (1993) *J. Biol. Chem.* **268,** 974–981
42. Wang, B., Pelletier, J., Massaad, M. J., Herscovics, A., and Shore, G. C. (2004) *Mol. Cell. Biol.* **24,** 2767–2778
43. Kahn, B. B., Simpson, I. A., and Cushman, S. W. (1988) *J. Clin. Invest.* **82,** 691–699
44. Zhang, H., Links, P. H., Ngsee, J. K., Tran, K., Cui, Z., Ko, K. W., and Yao, Z. (2004) *J. Biol. Chem.* **279,** 2221–2230
45. Livingstone, C., James, D. E., Rice, J. E., Hanpeter, D., and Gould, G. W. (1996) *Biochem. J.* **315,** 487–495
46. Belfort, G. M., Bakirtzi, K., and Kandror, K. V. (2005) *J. Biol. Chem.* **280,** 7262–7272
47. Shi, J., and Kandror, K. V. (2005) *Dev. Cell* **9,** 99–108
48. Garcia de Herreros, A., and Birnbaum, M. J. (1989) *J. Biol. Chem.* **264,** 19994–19999
49. Terrand, J., Bruban, V., Zhou, L., Gong, W., El Asmar, Z., May, P., Zurhove, K., Haffner, P., Philippe, C., Woldt, E., Matz, R. L., Gracia, C., Metzger, D., Auwerx, J., Herz, J., and Boucher, P. (2009) *J. Biol. Chem.* **284,** 381–388
50. Sano, H., Kane, S., Sano, E., Mîinea, C. P., Asara, J. M., Lane, W. S., Garner, C. W., and Lienhard, G. E. (2003) *J. Biol. Chem.* **278,** 14599–14602
51. Peck, G. R., Ye, S., Pham, V., Fernando, R. N., Macaulay, S. L., Chai, S. Y., and Albiston, A. L. (2006) *Mol. Endocrinol.* **20,** 2576–2583
52. Ramm, G., Larance, M., Guilhaus, M., and James, D. E. (2006) *J. Biol. Chem.* **281,** 29174–29180
53. Hosaka, T., Brooks, C. C., Presman, E., Kim, S. K., Zhang, Z., Breen, M., Gross, D. N., Sztul, E., and Pilch, P. F. (2005) *Mol. Biol. Cell* **16,** 2882–2890
54. Herz, J., Clouthier, D. E., and Hammer, R. E. (1992) *Cell* **71,** 411–421
55. Lillis, A. P., Van Duyn, L. B., Murphy-Ullrich, J. E., and Strickland, D. K. (2008) *Physiol. Rev.* **88,** 887–918
56. Corvera, S., Graver, D. F., and Smith, R. M. (1989) *J. Biol. Chem.* **264,** 10133–10138
57. Mîinea, C. P., Sano, H., Kane, S., Sano, E., Fukuda, M., Peränen, J., Lane, W. S., and Lienhard, G. E. (2005) *Biochem. J.* **391,** 87–93
58. Gotthardt, M., Trommsdorff, M., Nevitt, M. F., Shelton, J., Richardson, J. A., Stockinger, W., Nimpf, J., and Herz, J. (2000) *J. Biol. Chem.* **275,** 25616–25624
59. Shi, J., Huang, G., and Kandror, K. V. (2008) *J. Biol. Chem.* **283,** 30311–30321
60. Bonifacino, J. S., and Traub, L. M. (2003) *Annu. Rev. Biochem.* **72,** 395–447
61. Carvalho, E., Schellhorn, S. E., Zabolotny, J. M., Martin, S., Tozzo, E., Peroni, O. D., Houseknecht, K. L., Mundt, A., James, D. E., and Kahn, B. B. (2004) *J. Biol. Chem.* **279,** 21598–21605
62. Barile, M., Pisitkun, T., Yu, M. J., Chou, C. L., Verbalis, M. J., Shen, R. F., and Knepper, M. A. (2005) *Mol. Cell. Proteomics* **4,** 1095–1106
63. Bonifacino, J. S., and Hurley, J. H. (2008) *Curr. Opin Cell Biol.* **20,** 427–436
64. Brooks, C. C., Scherer, P. E., Cleveland, K., Whittemore, J. L., Lodish, H. F., and Cheatham, B. (2000) *J. Biol. Chem.* **275,** 2029–2036
65. Thoidis, G., Kotliar, N., and Pilch, P. F. (1993) *J. Biol. Chem.* **268,** 11691–11696
66. Huang, S., Lifshitz, L. M., Jones, C., Bellve, K. D., Standley, C., Fonseca, S., Corvera, S., Fogarty, K. E., and Czech, M. P. (2007) *Mol. Cell. Biol.* **27,** 3456–3469
67. Bai, L., Wang, Y., Fan, J., Chen, Y., Ji, W., Qu, A., Xu, P., James, D. E., and Xu, T. (2007) *Cell Metab.* **5,** 47–57
68. Rogaeva, E., Meng, Y., Lee, J. H., Gu, Y., Kawarai, T., Zou, F., Katayama, T., Baldwin, C. T., Cheng, R., Hasegawa, H., Chen, F., Shibata, N., Lunetta, K. L., Pardossi-Piquard, R., Bohm, C., Wakutani, Y., Cupples, L. A., Cuenco, K. T., Green, R. C., Pinessi, L., Rainero, I., Sorbi, S., Bruni, A., Duara, R., Friedland, R. P., Inzelberg, R., Hampe, W., Bujo, H., Song, Y. Q., Andersen, O. M., Willnow, T. E., Graff-Radford, N., Petersen, R. C., Dickson, D., Der, S. D., Fraser, P. E., Schmitt-Ulms, G., Younkin, S., Mayeux, R., Farrer, L. A., and St George-Hyslop, P. (2007) *Nat. Genet.* **39,** 168–177
69. Rappsilber, J., Ryder, U., Lamond, A. I., and Mann, M. (2002) *Genome Res.* **12,** 1231–1245
70. Nielsen, M. S., Jacobsen, C., Olivecrona, G., Gliemann, J., and Petersen, C. M. (1999) *J. Biol. Chem.* **274,** 8832–8836